Selective Imaging of Late Endosomes with a pH-Sensitive Diazaoxatriangulene Fluorescent Probe

Antoine Wallabregue,[†] Dimitri Moreau,[‡] Peter Sherin,[§,⊥] Pau Moneva Lorente,[†] Zdeňka Jarolímová,[#] Eric Bakker,*[#] Eric Vauthey,*[§] Jean Gruenberg,*[‡] and Jérôme Lacour*[†]

[†]Department of Organic Chemistry, [‡]Department of Biochemistry, [§]Department of Physical Chemistry, and [#]Department of Inorganic and Analytical Chemistry, University of Geneva, Quai Ernest Ansermet 30, 1211 Genève 4, Switzerland
[⊥]International Tomography Center SB RAS, Institutskaya street 3A, 630090 Novosibirsk, Russia

S *Supporting Information*

ABSTRACT: Late endosomes are a major trafficking hub in the cell at the crossroads between endocytosis, autophagy, and degradation in lysosomes. Herein is disclosed the first small molecule allowing their selective imaging and monitoring in the form of a diazaoxatriangulene fluorophore, **1a** (hexadecyl side chain). The compound is prepared in three steps from a simple carbenium precursor. In nanospheres, this pH-sensitive (pK_a = 7.3), photochemically stable dye fluoresces in the red part of visible light (601 and 578 nm, acid and basic forms, respectively) with a quantum yield between 14 and 16% and an excited-state lifetime of 7.7–7.8 ns. Importantly, the protonated form **1a·H⁺** provokes a specific staining of late endosome compartments (pH 5.0–5.5) after 5 h of incubation with HeLa cells. Not surprisingly, this late endosome marking depends on the intra-organelle pH, and changing the nature of the lipophilic chain provokes a loss of selectivity. Interestingly, fixation of the fluorophore is readily achieved with paraformaldehyde, giving the possibility to image both live and fixed cells.

Figure 1. (Top) pH-sensitive diazaoxatriangulene for late endosome staining: cationic **1a·H⁺** (hexadecyl side chain) and conjugated base **1a**. (Bottom) Previously reported cationic triangulene fluorophores (R = alkyl, aryl).

Scheme 1. Synthesis of Diazaoxatriangulenes Salts 1[a]

7a, R = C₁₆H₃₃	[1a·H⁺][PF₆], 36%	[1a·H⁺][TFA], 98%
7b, R = C₆H₅	[1b·H⁺][PF₆], 90%	[1b·H⁺][TFA], 97%
7c, R = C₃H₇	[1c·H⁺][PF₆], 94%	[1c·H⁺][TFA], 90%

[a]Reagents and conditions: (a) RNH₂ (3 equiv), CH₃CN, R = C₁₆H₃₃ or C₃H₇, 23 °C, 30 min or R = C₆H₅, 50 °C, 40 h; (b) H₂NNH₂·H₂O (25 equiv), 90 °C, 14 h; (c) molten pyrH⁺Cl⁻ (50 equiv), 150 °C, 4 h, then salt metathesis with a 2 M KPF₆ solution; (d) basification with NaHCO₃(aq) and then acidification with CF₃CO₂H (TFA, 1 M, aq).

Endocytosis,[1] the uptake of extracellular materials by cells, regulates fundamental cellular processes, including nutrient uptake and cholesterol homeostasis, immunity, signaling, adhesion, membrane turnover, and development. Consequently, the dysfunction of endocytotic organelles is associated with a number of diseases, in particular lysosomal storage disorders.[2] Endocytotic organelles, such as lysosomes, are thus intensively studied.[3] Their identification and characterization is usually achieved by fluorescence microscopy using antibodies coupled to fluorophores[4] or ectopically expressed proteins coupled to intrinsically fluorescent and genetically modified proteins (e.g., green fluorescent protein).[5] There is a growing need for rapid and noninvasive protocols based on small molecules (MW <500–600) to complement these techniques, for instance, for turn-on fluorescence or ratiomeric assays,[6] yet specificity is not easily obtained with small molecules. One of the main challenges is to achieve selective detection and imaging of the organelle of interest.[7] Herein, in a new development using lipophilic pH-sensitive diazaoxatriangulenes of type 1 (Figure 1 and Scheme 1), we report that late endosomes can be monitored selectively. These compounds,
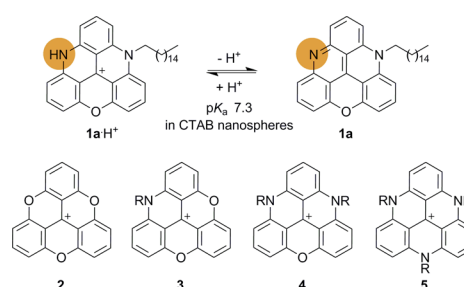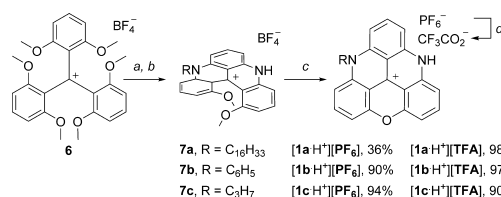
prepared in three steps from a simple carbenium precursor, are chemically and photochemically stable in micellar nanospheres in contact with water. Fluorescence occurs in the red part of the visible region (578–601 nm) with quantum yields varying from 13 to 16% and excited-state lifetimes between 6.5 and 7.8 ns. Interestingly, fixation of the fluorophore is readily achieved with paraformaldehyde, making it possible to image both live and fixed cells. All the data point to the importance of the basic nitrogen atom (pK_a = 7.3 in CTAB nanospheres for **1a·H⁺**) for both late endosome selectivity and fluorophore fixing.

In mammalian cells, all internalized molecules are delivered to early endosomes.[1b] From there, some lipids and proteins,

e.g., housekeeping receptors, are returned to the plasma membrane for re-utilization, while others, e.g., activated signaling receptors, are routed toward late endosomes and lysosomes for degradation. Late endosomes also function at a crossroad with autophagy, a pathway for the degradation and turnover of organelles and other cytosolic materials. The early endosome is acidified to pH ∼6.2 by the V-ATPase, allowing the uncoupling of bound ligands from their receptors.[8] By contrast, late endocytic organelles, late endosomes, and lysosomes are more acidic, with a luminal pH ∼5.0−5.5, which is required for the full activation of lysosomal hydrolases.

Previously, cationic triangulenes **2−5** (Figure 1) were studied for their impressive carbenium stability (pK_{R+} up to 23) and the variety of their chemical and (photo)physical properties.[9,10] A large range of applications from material sciences to biology have been developed.[9] In terms of bioimaging, lipophilic variants of **3** and **4** were studied with biorelevant DOPC vesicles.[11] In view of this result, it was decided to test triangulenes for organelle imaging and, to achieve high selectivity, to use the intra-organelle pH as a means for distinction.[4,12] However, as classical cationic triangulenes **2−5** are stable under acidic conditions and unresponsive to pH variations (2 < pH < 8), it was unlikely that these core structures would offer selectivity. Modifications were looked for, and derivatives **1a**, **1b**, and **1c**, containing a basic N-atom, were targeted (Scheme 1, R = hexadecyl, phenyl, and propyl, respectively). The synthesis was achieved in only three steps. Simple treatment of tris(2,6-dimethoxybenzene)methyl cation **6** with hexadecylamine, aniline, or propylamine, followed by reaction at 90 °C with excess hydrazine monohydrate, afforded **7a−c**.[13] Dissolution of these precursors in molten pyridinium hydrochloride (150 °C, 4 h) afforded the O-ring closure. Compounds **1a−c** were then isolated as their hexafluoro-phosphate salts after salt metathesis in modest to excellent yields (36−94%).

The optical properties of triangulene compounds as a function of acidity were characterized by absorption and fluorescence spectroscopy. Due to their high aromaticity and hydrophobicity, resulting in poor solubility and aggregation and subsequent precipitation of the neutral forms of **1a−c** in water, the compounds were incorporated into the hydrophobic core of polymeric nanospheres by a precipitation method reported earlier.[14] In addition to the functionalized triangulenes, the nanospheres were doped with lipophilic ion-exchanger dissolved in the nonpolar solvent bis(2-ethylhexyl) sebacate (Table S1). The protonation equilibrium is governed by ion exchange; see Scheme S1 and text in the Supporting Information (SI) for details.[15]

UV/vis and fluorescence spectroscopic analyses of the compounds were carried out between 300 and 800 nm over a broad pH range. To our satisfaction, protonation strongly affected the electronic structure and led to significant changes in the absorption and emission spectra (Figure 2A,B).[16] Similar spectral shifts were observed previously with a monoaza-triangulenium compound.[10a] A loss of vibronic structure and a red shift of both absorption and emission bands are observed upon protonation of the neutral form. The mirror-image symmetry of absorption and fluorescence spectra indicates one emissive state.[17] The aliphatic or aromatic nature of the side chain (R) has very little effect on the absorption spectra of the neutral forms (see Figures S11−S13); a similar lack of influence had been noticed in the quinacridines series **7**.[13]
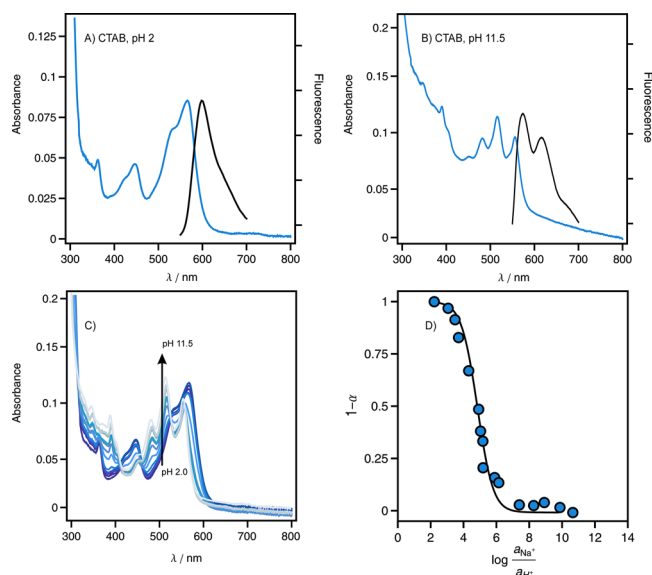

Figure 2. Electronic absorption (blue) and fluorescence (black) spectra recorded for ion-selective nanospheres encapsulating **1a** in CTAB (NP$_2$, see SI) in aqueous solutions at pH 2.0 (A) and 11.5 (B). Electronic absorption spectra at different pH (C) and ion-exchange dosage curve (D) fitted with eq 2 (see SI).

Figure 2C depicts the pH dependence of the absorption spectra (300−800 nm), and Figure 2D shows the specific absorbance at 575 nm for **1a**. The titration curves were analyzed assuming one acid/base equilibrium according to eq 2 in the SI. The pK_a values were determined using a recently introduced approach and are summarized in Table S2.[18] Electronic absorption spectra collected at different pH values for all examined triangulene compounds are shown in Figures S2−S4. The normalized absorbance changes with pH were corroborated with ion-exchange theory as explained in detail in the SI (Figures S5−S10).[15] Interestingly, the nature of the nitrogen substituent has an influence on the acidity: changing the hexadecyl chain (**1a**) to a phenyl or propyl group increases the pK_a value from 7.3 to 7.8 and 8.4 for **1a·H⁺**, **1b·H⁺**, and **1c·H⁺**, respectively, for the micellar system but decreases it from 9.5 to 9.3 and 8.5 for the pluronic F-127 system.[19] The differences in pK_a values for the two systems are ascribed to the solvent nature of the nanospheres.

The neutral diazaoxatriangulenes **1a,b** fluorescence near 580 nm, with a quantum yield (Φ_F) of 14% in micellar solution (Table S3). These Φ_F values are higher in organic solvents, varying between 20 and 40% (Table S3). Upon protonation, the emission band shifts to longer wavelength and peaks around 600 nm, yet protonation has a negligible effect on Φ_F of **1a,b** in the micellar solution.[20]

The fluorescence decays of protonated and neutral forms of **1a,b** were recorded at the maxima of emission bands by time-correlated single-photon counting upon excitation at 375 nm. These fluorescence decays could be well reproduced using a monoexponential function (Figure S15) with the time constants (τ_F) listed in Table S3 for organic solvents. Both Φ_F and τ_F values are higher for organic solvents than for micellar solutions. Significant isotopic effect indicates participation of intermolecular H-bonds in the acceleration of the nonradiative decay of the excited state for diazaoxa-triangulenes.[13,21] The photochemical stability of the protonated

and neutral forms of **1a** in acetonitrile was tested under anaerobic and aerobic conditions (Figure S16).[22]

With this information in hand, we examined the solubility of diazaoxatriangulenes $[1 \cdot H^+][PF_6]$ in biorelevant phosphate-buffered saline (PBS). Not too surprisingly, precipitation of the dyes was observed. This problem was partially solved by an anion-exchange metathesis. In fact, water-soluble fluorophores were obtained as protonated trifluoroacetate (TFA) salts. However, significant precipitation of the neutral form of dye could be observed after 1 h of staining in PBS solution at 0.3 mM concentration.[23] All derivatives $[1 \cdot H^+][PF_6]$ were converted in good yields (90−98%) to their corresponding TFA salts $[1 \cdot H^+][TFA]$ by washing with 1 M solutions of $NaHCO_3$ and subsequent acidification with CF_3CO_2H acid (Scheme S3).

Finally, to evaluate our initial hypothesis, HeLa cells were treated with the three salts $[1 \cdot H^+][TFA]$. Only with the more lipophilic derivative **1a** (R = $C_{16}H_{33}$) was a characteristic punctate staining observed by fluorescence microscopy (Figure 3A; nuclei are stained with DAPI). The fluorophore labeling colocalized to a very large extent with well-established markers of late endocytic compartments, the unconventional phospholipid lysobisphosphatidic acid (LBPA) detected with a monoclonal antibody and the transmembrane protein LAMP1.[1b] It is worth noting that **1a** staining intensity compares very nicely with that of LAMP1—a very abundant and highly antigenic component of late endocytic membranes. The staining was highly specific since little, if any, **1a** was found in structures lacking LBPA or LAMP1. Moreover, no colocalization could be observed between **1a** and the early endosomal marker EEA1 (Figure 3B).[24] After endosome segmentation and automated analysis, precise quantification of individual endosomes labeled with LAMP1 (90 × 10^3 endosomes in 2500 cells) or EEA1 (22 × 10^3 endosomes in 2100 cells) shows that **1a** is far more abundant in the former than in the latter endosomes (Figure 3D). Consistently a scatter plot of Ia integrated intensity per endosome correlates with the integrated intensity of the late (LAMP1) but not the early (EEA1) endosomal marker (Figure S23).

These data show that **1a** serves as a selective marker of late endocytic organelles. In fact, the staining was abolished after neutralization of the endosomal pH with the protonophore ionomycin, or with inhibitors of the V-ATPase[8a] concanamycin B or bafilomycin A1 (Figure 3C), demonstrating that **1a** accumulation is strictly dependent on the acidic environment of late endocytic organelles.[25] Upon protonation, **1a**·H^+ loses the capacity to freely cross membranes and accumulates in the acidic endosome lumen like other lysosomotropic compounds originally described by Christian de Duve.[26] While **1a** staining is easily detected without fixation in living cells (Figure 3C), the staining pattern was interestingly retained after fixation in paraformaldehyde (PFA) (Figure 3A,B). Hence, not only is **1a** selective for late endosomes, but, in contrast to most lysosomotropic dyes, it also serves as a fixable reporter of the pH in this organelle. In terms of photochemical stability, **1a** compares nicely with the other dyes used in this study, in vitro (Figure 3A,B) or in vivo (Figure 3C); this in accordance with recent studies using triangulenium dyes as cellular stains.[27] Finally, the dye is broadly applicable to any cell type with acidic late endosomes and lysosomes (Figure 3A−D in HeLa cells derived from a cervical cancer; Figure 3E shows A431 cells derived from epidermoid carcinoma), including all animal cells, and is compatible with most staining protocols and other
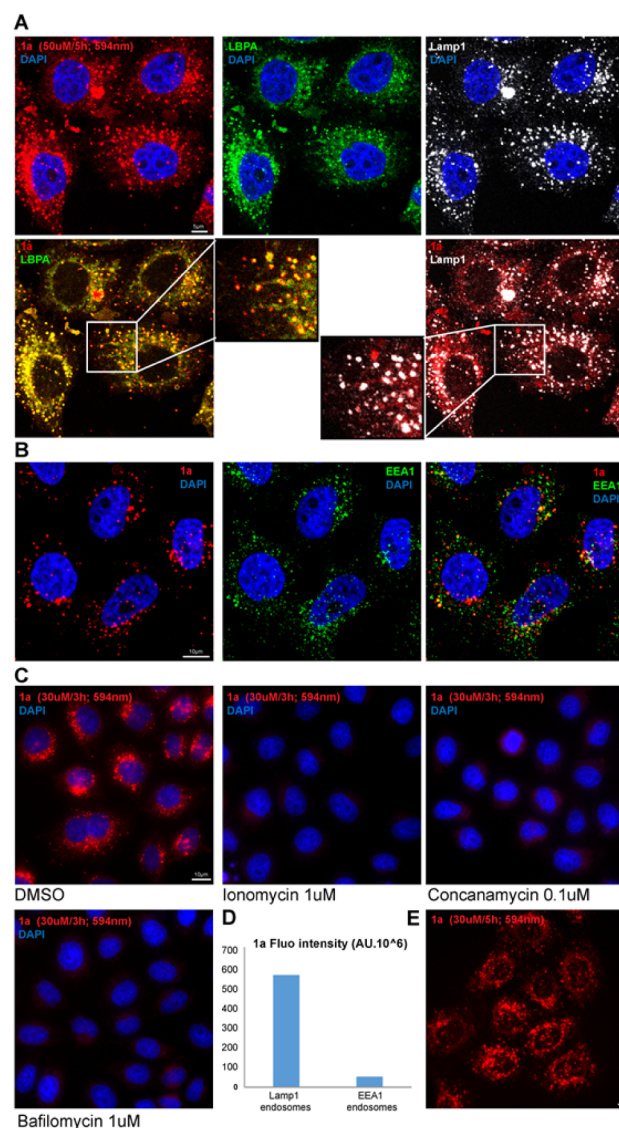

Figure 3. (A) HeLa cells treated with 50 μM solutions of $[1a \cdot H^+][TFA]$ for 5 h and fixed in PFA. The cells were then labeled with antibodies to LBPA and Lamp1, and then with secondary antibodies, and analyzed by fluorescence microscopy. Nuclei are stained with DAPI. (B) HeLa cells treated with 300 μM solutions of $[1a \cdot H^+][TFA]$ for 18 h were processed and analyzed as above using antibodies to EEA1. (C) HeLa cells treated for 3 h with 30 μM solutions of $[1a \cdot H^+][TFA]$ together with 1 μM ionomycin, 0.1 μM concanamycin B, or 1 μM bafilomycin A were analyzed live, without fixation, by fluorescence microscopy. (D) **1a** signal intensity quantification in Lamp1 or EEA1 masks. (E) A431 cells treated with **1a** and imaged under the same conditions.

biological markers (e.g., vital stains, antibodies, fluorescent proteins). To understand the molecular basis of this useful fixation mechanism, an experiment was performed. Compound **1a** (basic form) was added to a PBS solution containing 4% PFA. Interestingly, after only 10 min, a complete transformation of the UV/vis spectrum was achieved (Figure S20). The resulting spectrum is virtually superimposable to that of **1a**·H^+, despite the lack of pH change. This strongly indicates quaternization of the sp^2 nitrogen upon the addition of PFA. In fact, it is likely that a reaction between **1a** and PFA occurs to yield the corresponding pyridinium carbinol derivative; such

species are well established.[28] The resulting mixture displays the same absorption spectrum as **1a**·H$^+$.

In conclusion, we have shown that a diazaoxatriangulene fluorophore, readily prepared in three steps, allows selective imaging and monitoring of late endosomes. In water, luminescence is observed in the red part of visible light (>578 nm), with effective quantum yields (14−16%) and excited-state lifetimes (∼7.7 ns). The late endosome marking depends on the intraorganelle pH. Furthermore, fixation of the fluorophore is readily achieved with paraformaldehyde, giving the possibility to image both live and fixed cells.

■ ASSOCIATED CONTENT

Ⓢ Supporting Information

The Supporting Information is available free of charge on the ACS Publications website at DOI: 10.1021/jacs.5b09972.

> Synthetic procedures and spectral characterization of compounds **1** and related salts (PDF)

■ AUTHOR INFORMATION

Corresponding Authors

*eric.bakker@unige.ch; eric.vauthey@unige.ch; jean.gruenberg@unige.ch; jerome.lacour@unige.ch

Notes

The authors declare no competing financial interest.

■ ACKNOWLEDGMENTS

■ REFERENCES

(1) (a) McMahon, H. T.; Boucrot, E. *Nat. Rev. Mol. Cell Biol.* **2011**, *12*, 517. (b) Scott, C. C.; Vacca, F.; Gruenberg, J. *Semin. Cell Dev. Biol.* **2014**, *31*, 2. (c) Mukherjee, S.; Ghosh, R. N.; Maxfield, F. R. *Physiol. Rev.* **1997**, *77*, 759.

(2) Futerman, A. H.; van Meer, G. *Nat. Rev. Mol. Cell Biol.* **2004**, *5*, 554.

(3) (a) Peña, B.; Barhoumi, R.; Burghardt, R. C.; Turro, C.; Dunbar, K. R. *J. Am. Chem. Soc.* **2014**, *136*, 7861. (b) Sun, R.; Liu, W.; Xu, Y.-J.; Lu, J.-M.; Ge, J.-F.; Ihara, M. *Chem. Commun.* **2013**, *49*, 10709. (c) Zhu, H.; Fan, J.; Xu, Q.; Li, H.; Wang, J.; Gao, P.; Peng, X. *Chem. Commun.* **2012**, *48*, 11766. (d) Yin, L.; He, C.; Huang, C.; Zhu, W.; Wang, X.; Xu, Y.; Qian, X. *Chem. Commun.* **2012**, *48*, 4486. (e) Li, Z.; Song, Y.; Yang, Y.; Yang, L.; Huang, X.; Han, J.; Han, S. *Chem. Sci.* **2012**, *3*, 2941. (f) Fan, L.; Fu, Y.-J.; Liu, Q.-L.; Lu, D.-T.; Dong, C.; Shuang, S.-M. *Chem. Commun.* **2012**, *48*, 11202.

(4) Urano, Y.; Asanuma, D.; Hama, Y.; Koyama, Y.; Barrett, T.; Kamiya, M.; Nagano, T.; Watanabe, T.; Hasegawa, A.; Choyke, P. L.; Kobayashi, H. *Nat. Med.* **2009**, *15*, 104.

(5) Miesenbock, G.; De Angelis, D. A.; Rothman, J. E. *Nature* **1998**, *394*, 192.

(6) Han, J.; Burgess, K. *Chem. Rev.* **2010**, *110*, 2709.

(7) (a) Sampedro, A.; Villalonga-Planells, R.; Vega, M.; Ramis, G.; Fernandez de Mattos, S.; Villalonga, P.; Costa, A.; Rotger, C. *Bioconjugate Chem.* **2014**, *25*, 1537. (b) Soulet, D.; Gagnon, B.; Rivest, S.; Audette, M.; Poulin, R. *J. Biol. Chem.* **2004**, *279*, 49355.

(8) (a) Scott, C. C.; Gruenberg, J. *BioEssays* **2011**, *33*, 103. (b) Marshansky, V.; Futai, M. *Curr. Opin. Cell Biol.* **2008**, *20*, 415.

(9) Bosson, J.; Gouin, J.; Lacour, J. *Chem. Soc. Rev.* **2014**, *43*, 2824 and references therein.

(10) (a) Laursen, W. B.; Krebs, C. F. *Chem.-Eur. J.* **2001**, *7*, 1773. (b) Laursen, B. W.; Krebs, F. C. *Angew. Chem., Int. Ed.* **2000**, *39*, 3432. (c) Laursen, B. W.; Krebs, F. C.; Nielsen, M. F.; Bechgaard, K.; Christensen, J. B.; Harrit, N. *J. Am. Chem. Soc.* **1998**, *120*, 12255. (d) Martin, J. C.; Smith, R. G. *J. Am. Chem. Soc.* **1964**, *86*, 2252.

(11) Maliwal, B. P.; Fudala, R.; Raut, S.; Kokate, R.; Sorensen, T. J.; Laursen, B. W.; Gryczynski, Z.; Gryczynski, I. *PLoS One* **2013**, *8*, e63043.

(12) (a) Lee, H.; Akers, W.; Bhushan, K.; Bloch, S.; Sudlow, G.; Tang, R.; Achilefu, S. *Bioconjugate Chem.* **2011**, *22*, 777. (b) Han, J.; Burgess, K. *Chem. Rev.* **2010**, *110*, 2709. (c) Hilderbrand, S. A.; Kelly, K. A.; Niedre, M.; Weissleder, R. *Bioconjugate Chem.* **2008**, *19*, 1635. (d) Hilderbrand, S. A.; Weissleder, R. *Chem. Commun.* **2007**, 2747.

(13) Wallabregue, A.; Sherin, P.; Guin, J.; Besnard, C.; Vauthey, E.; Lacour, J. *Eur. J. Org. Chem.* **2014**, *2014*, 6431.

(14) Xie, X.; Mistlberger, G.; Bakker, E. *Anal. Chem.* **2013**, *85*, 9932.

(15) Bakker, E.; Buhlmann, P.; Pretsch, E. *Chem. Rev.* **1997**, *97*, 3083.

(16) Absorption and emission spectra were also recorded for both protonated and neutral forms of **1a,b** in various organic solvents; see Figure S14. Increasing solvent polarity and H-bond donor ability gives rise to monotonic but modest bathochromic shifts (∼10 nm) of both absorption and emission spectra of **1a,b**. However, no clear influence of these solvent parameters on the spectral properties of **1a**·H$^+$ and **1b**·H$^+$ can be seen.

(17) This is supported by the fluorescence excitation spectra, which exhibit full coincidence with the absorption spectra; see Figure S19.

(18) Xie, X.; Zhai, J.; Jarolímová, Z.; Bakker, E., 2016, submitted.

(19) Preliminary DFT calculations indicate that the HOMO orbitals and charge distributions of **1a−c** (and their conjugated acids **1**·H$^+$) are very similar. The observed variation of the apparent pK_a value with different side chains is likely a manifestation of their different polarity and thus their interaction with the solvent environment.

(20) This is not the case with organic solvents, as protonation leads to an increase of ∼20% of the Φ_F values; see Table S3.

(21) (a) Richert, S.; Mosquera Vazquez, S.; Grzybowski, M.; Gryko, D. T.; Kyrychenko, A.; Vauthey, E. *J. Phys. Chem. B* **2014**, *118*, 9952. (b) Kel, O.; Sherin, P.; Mehanna, N.; Laleu, B.; Lacour, J.; Vauthey, E. *Photochem. Photobiol. Sci.* **2012**, *11*, 623. (c) Fita, P.; Fedoseeva, M.; Vauthey, E. *J. Phys. Chem. A* **2011**, *115*, 2465. (d) Sherin, P. S.; Grilj, J.; Tsentalovich, Y. P.; Vauthey, E. *J. Phys. Chem. B* **2009**, *113*, 4953.

(22) The stability of solutions of [**1a**·H$^+$][TFA] with respect to aggregation and precipitation was also investigated in various solvent conditions; see Figures S17 and S18.

(23) Aggregation of **1a** neutral form is slowed down by the presence of DMSO and negligible in the case of pure organic solvent like CH$_3$CN. In the presence of water, **1a** finally forms snowflake-like structures.

(24) Simonsen, A.; Lippe, R.; Christoforidis, S.; Gaullier, J. M.; Brech, A.; Callaghan, J.; Toh, B. H.; Murphy, C.; Zerial, M.; Stenmark, H. *Nature* **1998**, *394*, 494.

(25) As such, it is likely that the active form of **1a** is the conjugated acid form **1a**·H$^+$.

(26) De Duve, C.; De Barsy, T.; Poole, B.; Trouet, A.; Tulkens, P.; Van Hoof, F. O. *Biochem. Pharmacol.* **1974**, *23*, 2495.

(27) (a) Sørensen, T. J.; Thyrhaug, E.; Szabelski, M.; Luchowski, R.; Gryczynski, I.; Gryczynski, Z.; Laursen, B. W. *Methods Appl. Fluoresc.* **2013**, *1*, 025001. (b) Bogh, S. A.; Bora, I.; Rosenberg, M.; Thyrhaug, E.; Laursen, B. W.; Sørensen, T. J. *Methods Appl. Fluoresc.* **2015**, *3*, 045001. (c) Bora, I.; Bogh, S. A.; Santella, M.; Rosenberg, M.; Sørensen, T. J.; Laursen, B. W. *Eur. J. Org. Chem.* **2015**, *2015*, 6351. (d) Shivalingam, A.; Izquierdo, M. A.; Marois, A. L.; Vysniauskas, A.; Suhling, K.; Kuimova, M. K.; Vilar, R. *Nat. Commun.* **2015**, *6*, 8178. (e) Bora, I.; Bogh, S. A.; Rosenberg, M.; Santella, M.; Sorensen, T. J.; Laursen, B. W. *Org. Biomol. Chem.* **2016**, *14*, 1091.

(28) (a) Mistry, D.; Powles, N.; Page, M. I. *J. Org. Chem.* **2013**, *78*, 10732. (b) Kahn, K.; Bruice, T. C. *J. Am. Chem. Soc.* **2001**, *123*, 11960.